THE EFFECTS OF THE NODAL REGRESSION OF THE ORBIT ON THE GRAVITY PRECESSION OF A GYROSCOPIC SATELLITE

James L. Myers, Jr.

REPORT R-309   JULY, 1966

NOTATION

A	Moment of inertia about transverse axes
a	Semi-major axis of ellipse
$\hat{a}_1$, $\hat{a}_2$	Unit vectors
C	Polar moment of inertia
e	Eccentricity of orbit
G	Universal gravitational constant
$\underline{H}$	Angular momentum vector
i	Orbital inclination; angle measured from earth's polar axis to orbital angular velocity vector
$\hat{i}$, $\hat{j}$, $\hat{k}$	Unit vectors in inertial coordinate system
M	Mass of the earth
M_x, M_y, M_z	Components of gravity gradient moment
R	Radius from center of earth to center of satellite
R_e	Radius of earth
T	Orbital period
t	Time
x, y, z	Coordinate axes
α	Argument of perigee in orbital plane
δ_e	Spin axis error angle for equatorial orbit (small)
δ_p	Spin axis error angle for polar orbit
ϵ	Gyro spin axis inclination
η	Coordinate transformation angle
θ	Angle between gyro spin axis and orbital angular velocity vector

Λ Gravity gradient precession coefficient

φ Right ascension of gyro; angle measured west-to-east in earth's equatorial plane from the vernal equinox to the line of nodes between gyro and earth equatorial planes

Ψ Argument of satellite in orbital plane

Ω Right ascension of orbit

$\underline{\omega}$ Angular velocity vector of gyro precession

$\underline{\omega}_o$ Orbital angular velocity vector

$\underline{\omega}_s$ Gyro spin axis vector

$\wedge$ Denotes unit vector

A gyroscopic satellite has been proposed for a test of the general theory of relativity[1,2] in which the gyro "drift" rate to be measured is less than seven seconds of arc per year. The Coordinated Science Laboratory has proposed a simple passive gyroscope which uses sunlight reflected from mirrors to provide optical data to determine the spin axis orientation.[3,4] The gravity gradient torque acting on the satellite is one of several extraneous disturbances which can cause spurious precession of the gyro spin axis. In this paper, general equations for the precession of a gyro satellite in a regressing orbit are derived. These equations may be used to specify the tolerances for initial spin axis and orbit alignments which enable an accurate measurement of the relativity effect.

1. Gravity Gradient Moment

The gravity gradient moment is given by ref. 5 for the fixed orbit configuration shown in Fig. 1. Two coordinate systems are shown, system [2] fixed to the body spin axis, $\underline{\omega}_s$, and system [3] fixed to the orbital plane, or to the orbital angular velocity vector, $\underline{\omega}_o$. The x_2 axis is the line of nodes between the orbital $(x_3 - y_3)$ plane and the equatorial $(x_2 - y_2)$ plane of the orbiting gyro. The gravity gradient moment components in the body axis system given in ref. 5 are

$$
\left.
\begin{aligned}
M_{x_2} &= -\frac{3GM}{R^3}(C-A)\sin\theta\cos\theta\sin^2\omega_o t \\[2mm]
M_{y_2} &= -\frac{3}{2}\frac{GM}{R^3}(C-A)\sin\theta\sin 2\omega_o t \\[2mm]
M_{z_2} &= 0
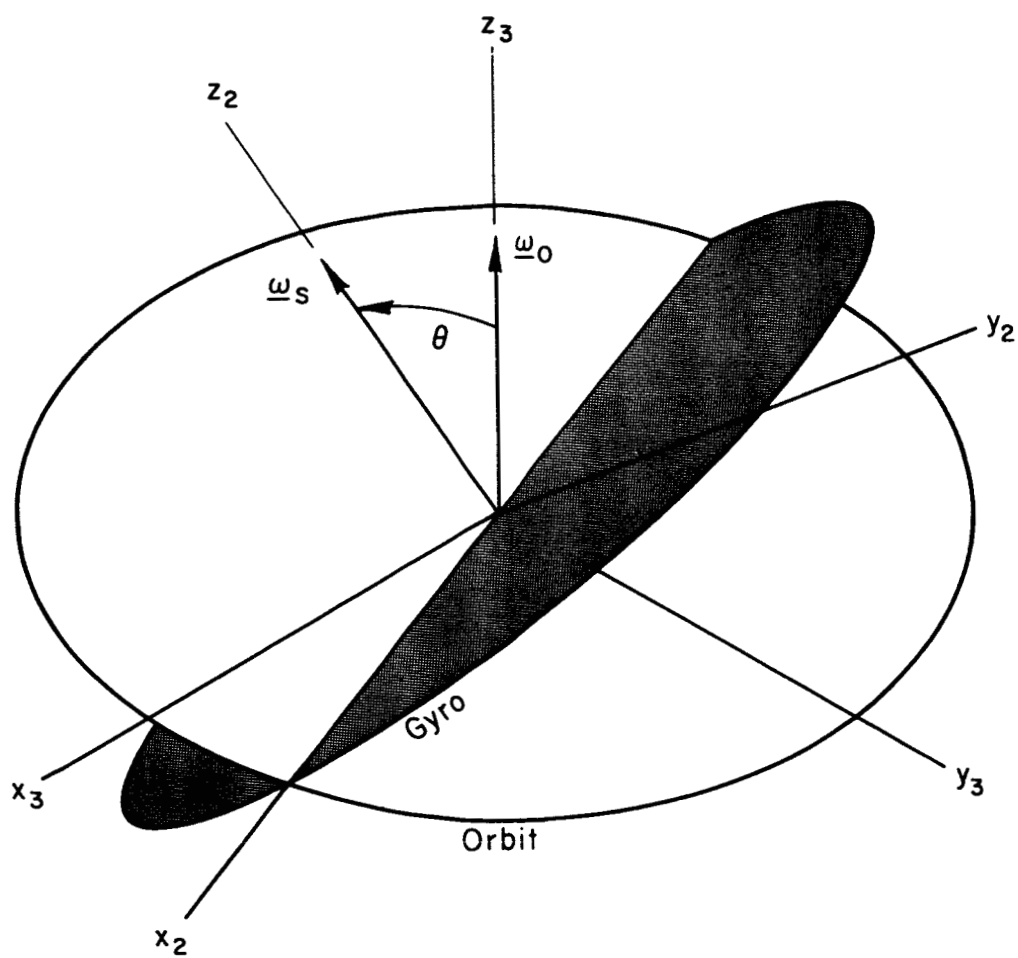\end{aligned}
\right\}
\qquad (1)
$$

Fig. 1   Planes of gyro equator and orbit;
          coordinate systems [2] and [3].

where M is the mass of the earth and R is the distance between the centers of the satellite and the earth. θ is the angle between the vectors $\underline{\omega}_s$ and $\underline{\omega}_o$, and varies only because of precession of $\underline{\omega}_s$. In the general case the satellite's orbital plane will regress about the earth's polar axis at the rate of $\dot{\Omega}$ degrees per year[6] and will produce an additional change in θ.

The geometry involved in the general case of interest for regressing orbits is illustrated in Fig. 2. An earth-based coordinate system is fixed with z_o along the earth's north pole and x_o along the line of vernal equinox (i.e., the line of the nodes between the ecliptic and the earth's equatorial plane). The y_o axis completes an orthogonal right-handed system and therefore, lies in the earth's equatorial plane. Systems [2] and [3] bear the same relationship to each other as shown in Fig. 1. A new coordinate system, [1], is shown with z_1 also along the gyro spin axis, but with x_1 along the line of nodes between the earth's and gyro's equatorial planes. This is the most logical system to observe gyro motion with respect to the earth. The moment given for system [2] can be transformed through angle η to system [1] by the transformation

$$\begin{bmatrix} \cos\eta & -\sin\eta & 0 \\ \sin\eta & \cos\eta & 0 \\ 0 & 0 & 1 \end{bmatrix}.$$

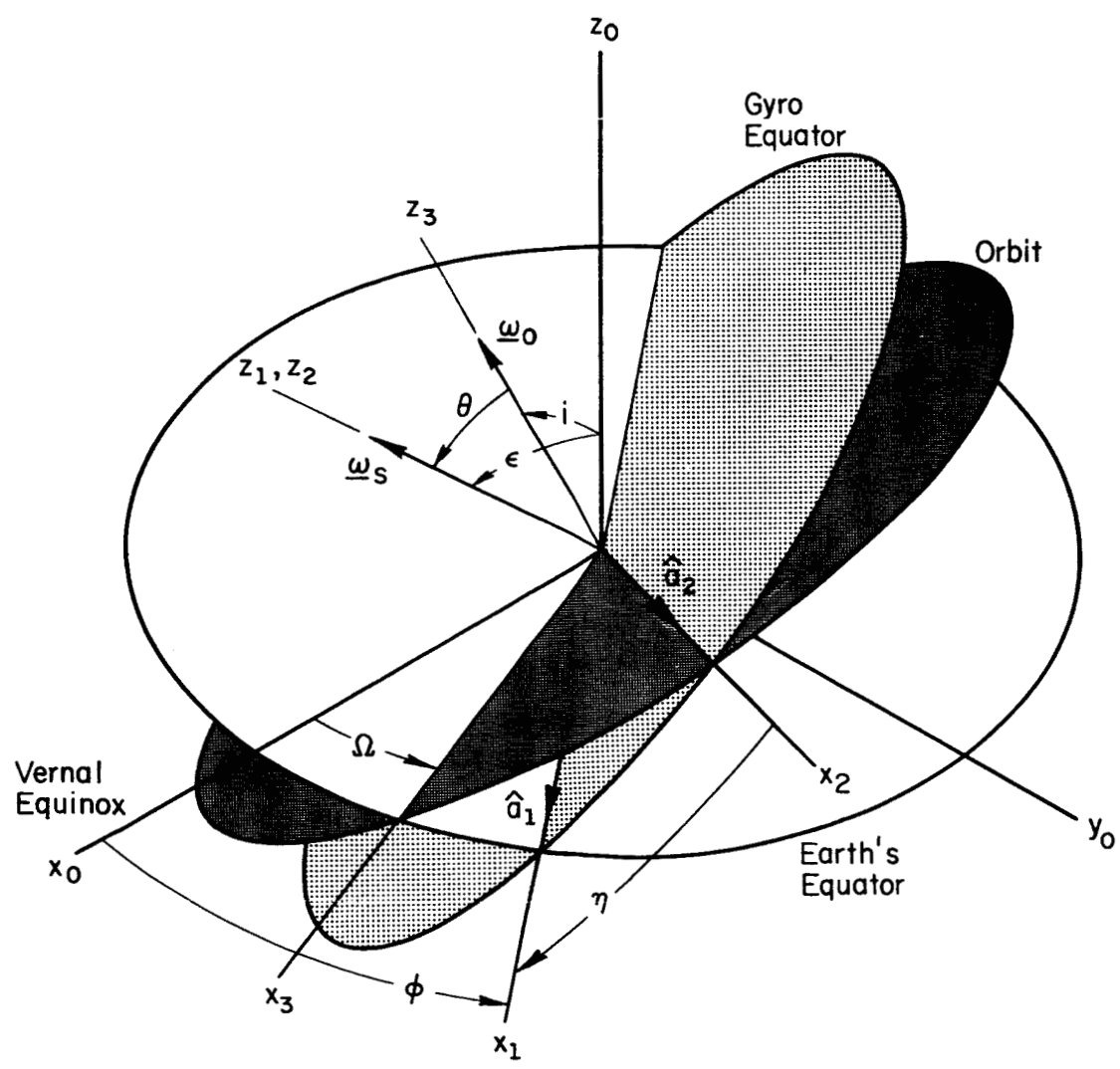The moment components in system [1] are now given by

Fig. 2   Orbit and gyro frames related to inertial
          system; coordinate systems [0], [1], [2], [3].

$$M_{x_1} = \cos\eta \; M_{x_2} - \sin\eta \; M_{y_2}$$

$$M_{y_1} = \sin\eta \; M_{x_2} + \cos\eta \; M_{y_2}$$

$$M_{z_1} = M_{z_2} = 0 \; .$$

Substituting the values for M_{x_2} and M_{y_2} gives

$$M_{x_1} = - \frac{3GM}{R^3} \; (C-A) \; \cos\eta \; \sin\theta \; \cos\theta \; \sin^2 \omega_o t$$

$$+ \frac{3}{2} \frac{GM}{R^3} \; (C-A) \; \sin\eta \; \sin\theta \; \sin 2\omega_o t$$

(2)

$$M_{y_1} = - \frac{3GM}{R^3} \; (C-A) \; \sin\eta \; \sin\theta \; \cos\theta \; \sin^2 \omega_o t$$

$$- \frac{3}{2} \frac{GM}{R^3} \; (C-A) \; \cos\eta \; \sin\theta \; \sin 2\omega_o t.$$

(3)

$\cos\theta$, $\cos\eta \; \sin\theta$, and $\sin\eta \; \sin\theta$ will now be found as functions of i, Ω, $\in$, and φ. From Fig. 2, the gyro spin axis unit vector is given as

$$\hat{\omega}_s = \sin\in \; \sin\varphi \hat{i} - \sin\in \; \cos\varphi \hat{j} + \cos\in \hat{k},$$

(4)

and the orbital angular velocity unit vector is

$$\hat{\omega}_o = \sin i \; \sin\Omega \hat{i} - \sin i \; \cos\Omega \hat{j} + \cos i \hat{k}.$$

(5)

Therefore, $\cos\theta = \hat{\omega}_s \cdot \hat{\omega}_o$

$$= \sin i \; \sin\in \; \cos(\Omega-\varphi) + \cos i \; \cos \in.$$

(6)

From Fig. 2 a unit vector $\hat{a}_1$ is defined along x_1:

$$\hat{a}_1 = \cos\varphi \hat{i} + \sin\varphi \hat{j}.$$

From Fig. 2 it is seen that the x_2 axis is the line of nodes between the gyro equatorial plane and the orbital plane. Therefore, the x_2 axis is normal to both $\hat{\omega}_s$ and $\hat{\omega}_o$, and a new vector along x_2 may be defined:

$$\underline{a}_2 \equiv \hat{\omega}_o \times \hat{\omega}_s = \sin\theta \, \hat{a}_2 .$$

Now

$$\hat{a}_1 \cdot \underline{a}_2 = a_2 \cos\eta = \sin\theta \cos\eta$$

or

$$\cos\eta \sin\theta = \hat{a}_1 \cdot \hat{\omega}_o \times \hat{\omega}_s$$

$$= - \sin i \cos\epsilon \cos(\Omega-\varphi) + \cos i \sin\epsilon . \qquad (7)$$

Also it can be seen that

$$\hat{a}_1 \times \underline{a}_2 = a_2 \sin\eta \, \hat{\omega}_s$$

$$= \sin\theta \sin\eta \, \hat{\omega}_s$$

or

$$\sin\eta \sin\theta \, \hat{\omega}_s = \hat{a}_1 \times (\hat{\omega}_o \times \hat{\omega}_s)$$

$$= (\hat{a}_1 \cdot \hat{\omega}_s) \hat{\omega}_o - (\hat{a}_1 \cdot \hat{\omega}_o) \hat{\omega}_s .$$

But,

$$\hat{a}_1 \cdot \hat{\omega}_s = 0,$$

therefore,

$$\sin\eta \sin\theta = - (\hat{a}_1 \cdot \hat{\omega}_o) .$$

Substitution of the vector components yields

$$\sin\eta \sin\theta = - \sin i \sin(\Omega-\varphi) . \qquad (8)$$

Equations (7) and (8) can now be substituted into the moment equations (2) and (3):

$$M_{x_1} = \frac{3GM}{R^3} (C-A)[\sin i \cos \epsilon \cos(\Omega - \varphi) - \cos i \sin \epsilon] \cos \theta \sin^2 \omega_o t$$

$$- \frac{3}{2} \frac{GM}{R^3} (C-A) \sin i \sin(\Omega - \varphi) \sin 2\omega_o t \qquad (9)$$

$$M_{y_1} = 3 \frac{GM}{R^3} (C-A) \sin i \sin(\Omega - \varphi) \cos \theta \sin^2 \omega_o t$$

$$+ \frac{3}{2} \frac{GM}{R^3} (C-A)[\sin i \cos \epsilon \cos(\Omega - \varphi) - \cos i \sin \epsilon] \sin 2\omega_o t \qquad (10)$$

$$M_{z_1} = 0 . \qquad (11)$$

These equations give the gravity gradient moment for a given set of orbital parameters, i and Ω, and gyro spin direction ϵ and φ.

2. Precession

The precession rate $\underline{\omega}$ of coordinate system [1] can be found from Euler's dynamical equation

$$\underline{\dot{H}} + \underline{\omega} \times \underline{H} = \underline{M}. \qquad (12)$$

By inspection of Fig. 2, the components of $\underline{\omega}$ in system [1] are written

$$\omega_{x_1} = \dot{\epsilon}$$

$$\omega_{y_1} = \dot{\varphi} \sin \epsilon$$

$$\omega_{z_1} = \dot{\varphi} \cos \epsilon .$$

Since the coordinate axes of system [1] lie along the principal axes of the body, the angular momentum vector $\underline{H}$ and its derivative are given as

$$H_{x_1} = A \dot{\epsilon}$$

$$H_{y_1} = A \dot{\varphi} \sin \epsilon$$

$$H_{z_1} = C(\omega_s + \dot{\varphi} \cos \epsilon)$$

and

$$\dot{H}_{x_1} = A \ddot{\epsilon}$$

$$\dot{H}_{y_1} = A(\ddot{\varphi} \sin \epsilon + \dot{\varphi} \dot{\epsilon} \sin \epsilon)$$

$$\dot{H}_{z_1} = C(\dot{\omega}_s + \ddot{\varphi} \cos \epsilon - \dot{\varphi} \dot{\epsilon} \sin \epsilon).$$

Upon substitution of these components into Eq. (12) we have

$$
\left.
\begin{aligned}
A\ddot{\epsilon} + C\omega_s \dot{\varphi} \sin \epsilon + (C-A) \dot{\varphi}^2 \sin \epsilon \cos \epsilon &= M_{x_1} \\
(2A - C) \dot{\varphi} \dot{\epsilon} \cos \epsilon + A\ddot{\varphi} \sin \epsilon - C\omega_s \dot{\epsilon} &= M_{y_1} \\
C(\dot{\omega}_s + \ddot{\varphi} \cos \epsilon - \dot{\varphi} \dot{\epsilon} \sin \epsilon) &= M_{z_1}
\end{aligned}
\right\}
\qquad (13)
$$

The angular rate of the gyro, ω_s, typically is more than ten orders of magnitude larger than $\dot{\varphi}$ or $\dot{\epsilon}$. As will be seen later, $\ddot{\varphi}$ and $\ddot{\epsilon}$ are of the order of $\dot{\varphi}^2$ or $\dot{\epsilon}^2$. Therefore, Eqs. (13) may be simplified by neglecting all terms on the left-hand side which do not contain the factor ω_s. Now it can be seen that

$$\dot{\varphi} = \frac{M_{x_1}}{C\omega_s \sin \epsilon} \qquad (14)$$

$$\dot{\epsilon} = - \frac{M_{y_1}}{C\omega_s} \qquad (15)$$

$$\dot{\omega}_s = \dot{\varphi} \dot{\epsilon} \sin \epsilon - \ddot{\varphi} \cos \epsilon. \qquad (16)$$

Substituting Eqs. (9) and (10) into (14) and (15) gives

$$\dot{\varphi} = \frac{3GM}{R^3 \omega_s} \left(\frac{C-A}{C}\right) \{[\sin i \cot \epsilon \cos(\Omega-\varphi) - \cos i]\cos\theta \sin^2 \omega_o t$$

$$+ \frac{1}{2} \frac{\sin i}{\sin \epsilon} \sin(\Omega-\varphi) \sin 2\omega_o t\} \tag{17}$$

$$\dot{\epsilon} = \frac{3GM}{R^3 \omega_s} \left(\frac{C-A}{C}\right) \{\sin i \sin(\Omega-\varphi) \cos\theta \sin^2 \omega_o t$$

$$- \frac{1}{2} [\sin i \cos \epsilon \cos(\Omega-\varphi) - \cos i \sin \epsilon] \sin 2\omega_o t\} \tag{18}$$

where $\cos\theta$ is given by Eq. (6).

Assuming that i, Ω, ϵ, and φ change much less rapidly than $\omega_o t$, average rates $\tilde{\dot{\varphi}}$ and $\tilde{\dot{\epsilon}}$ may be found by integrating over one orbital period

$$\tilde{\dot{\varphi}} = \frac{1}{T} \int_o^T \dot{\varphi} dt$$

$$\tilde{\dot{\epsilon}} = \frac{1}{T} \int_o^T \dot{\epsilon} dt.$$

For an elliptical orbit, the radius R from the center of the earth is

$$R = \frac{a(1-e^2)}{1 + e \cos(\Psi-\alpha)}$$

where a = semi major axis of the ellipse

e = eccentricity

$\Psi = \omega_o t$ = argument of the satellite

α = argument of perigee.

Also, Kepler's law of areas provides the relation

$$R^2 \dot{\Psi} = \sqrt{GM\ a(1-e^2)}$$

therefore,

$$\frac{dt}{R^3} = \frac{dt}{R\ R^2 \frac{d\Psi}{dt}} \cdot \frac{d\Psi}{dt} = \frac{d\Psi}{\sqrt{GM\ a(1-e^2)}\ R} \ .$$

Now, integration of (17) over one orbital period becomes an integration

from 0 to 2π in Ψ:

$$\tilde{\phi} = \frac{3\ GM}{\sqrt{GM\ a(1-e^2)}}\ \frac{C-A}{C\omega_s}\ \{[\sin i\ \cot\varepsilon\ \cos(\Omega-\phi) - \cos i]\cos\theta$$

$$\frac{1}{a(1-e^2)T} \int_0^{2\pi} \sin^2\Psi[1 + e(\cos\Psi\ \cos\alpha + \sin\Psi\ \sin\alpha)]d\Psi$$

$$+ \frac{\sin i}{\sin\varepsilon}\ \frac{\sin(\Omega-\phi)}{a(1-e^2)T} \int_0^{2\pi} \sin\Psi\ \cos\Psi[1 + e(\cos\Psi\ \cos\alpha + \sin\Psi\ \sin\alpha)]d\Psi\}.$$

The first integral yields π, and the second integral vanishes. Equation

(18) is integrated similarly, and the resulting time averages are

$$\tilde{\phi} = \Lambda[\sin i\ \cot\varepsilon\ \cos(\Omega-\phi) - \cos i]\cos\theta \tag{19}$$

$$\tilde{\varepsilon} = \Lambda[\sin i\ \sin(\Omega-\phi)]\cos\theta \tag{20}$$

where the gravity gradient precession coefficient is defined as

$$\Lambda \equiv \frac{3}{2}\ \frac{GM}{a^3(1-e^2)^{3/2}}\ \frac{C-A}{C\omega_s}.$$

The orbital period T, has been eliminated by the equation

$$T = \frac{2\pi\ a^{3/2}}{\sqrt{GM}}\ .$$

Equations (19) and (20) may be integrated with respect to time for any i(t) and $\Omega(t)$ to give φ and $\in$ as functions of time. $\tilde{\varphi}$ and $\tilde{\in}$ are both of the order of Λ, and therefore, this quantity must be small (specifically, $\frac{\Lambda}{\omega_s} \ll 1$) for the foregoing derivation to be valid. Furthermore, the time derivatives of (19) and (20) show that $\dot{\tilde{\varphi}}$, $\dot{\tilde{\in}}$, and therefore $\dot{\omega}_s$ are of the order $\tilde{\varphi}^2$ or $\tilde{\in}^2$, as assumed previously.

3. Special Orbits

The relativity drift rate of the gyro spin axis will be largest when the spin axis lies in the orbital plane.[1] Therefore, two cases of special interest are an equatorial orbit and a polar orbit, because either of these orbits will allow the gyro spin axis to lie in the orbital plane for an extended period of time. For each of these special cases, Eqs. (19) and (20) may be simplified and integrated directly, as will be seen.

A. Equatorial Orbit

For an equatorial orbit, the inclination i will be assumed small so that
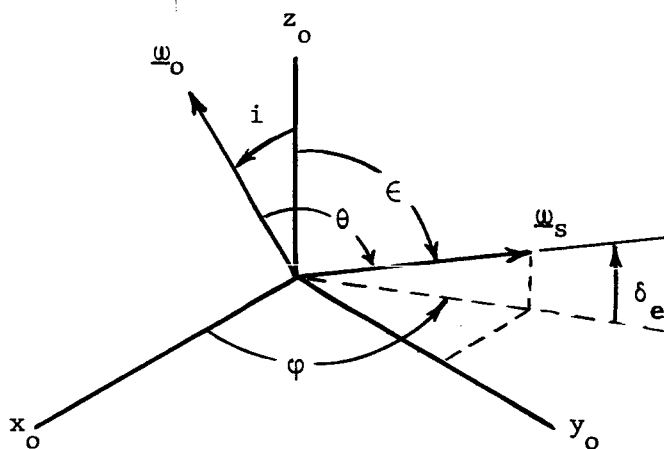
$$\sin i \approx i,$$
$$\cos i \approx 1.$$

Also, it is assumed that

$$\in = \frac{\pi}{2} + \delta_e,$$

where δ_e is a small angle between the spin axis and the x_o - y_o plane, as shown in the sketch.

Now,

$$\sin \epsilon = \sin(\frac{\pi}{2} + \delta_e) = \cos \delta_e \approx 1 \tag{21}$$

$$\cos \epsilon = \cos(\frac{\pi}{2} + \delta_e) = -\sin \delta_e \approx -\delta_e . \tag{22}$$

From Eq. (6)

$$\cos \theta = \sin i \cos(\Omega-\varphi) - \delta_e \cos i .$$

Since i is also a small angle,

$$\cos \theta \approx i \cos(\Omega-\varphi) - \delta_e . \tag{23}$$

Substituting Eqs. (21) to (23) into Eqs. (19) and (20) results in the following

$$\tilde{\varphi} = - \Lambda \Big[i^2 \delta_e \cos^2(\Omega-\varphi) + i \delta_e^2 \cos(\Omega-\varphi)$$

$$+ i \cos(\Omega-\varphi) - \delta_e \Big]$$

$$\tilde{\epsilon} = \Lambda \Big[\frac{i^2}{2} \sin 2(\Omega-\varphi) - i \delta_e \sin(\Omega-\varphi) \Big] .$$

Since i and δ_e are both small, $\tilde{\dot{\varphi}}$ is larger by at least one order of magnitude than $\tilde{\dot{\epsilon}}$, and may now be simplified by dropping the higher order terms in i and δ_e:

$$\tilde{\dot{\varphi}} \approx \Lambda [\delta_e - i \cos(\Omega-\varphi)]. \tag{24}$$

For near equatorial orbits, Ω changes at the rate of 6 to 9 revolutions per year. Therefore, Eq. (24) indicates that the average rate of change of φ is proportional to δ_e, the angle between the gyro spin axis and the earth's equatorial plane. Setting $\Omega = \Omega_o + \dot{\Omega}t$, Eq. (24) can be integrated with respect to time to give $\Delta\varphi$:

$$\Delta\varphi = \Lambda \left\{ \delta_e - i \left[\cos(\Omega_o - \varphi) \frac{\sin \dot{\Omega}t}{\dot{\Omega}t} + \sin(\Omega_o - \varphi) \frac{(\cos \dot{\Omega}t-1)}{\dot{\Omega}t} \right] \right\} t.$$

By arbitrarily setting $\Omega_o - \varphi = \frac{\pi}{2}$, this simplifies to

$$\Delta\varphi = \Lambda \left[\delta_e + i\left(\frac{1 - \cos \dot{\Omega}t}{\dot{\Omega}t}\right) \right] t . \tag{25}$$

From Eq. (25) it is seen that for large values of $\dot{\Omega}t$, $\Delta\varphi$ is proportional to δ_e.

B. Polar Orbit

A true polar orbit (i.e., $i = \frac{\pi}{2}$) is required for a nonregressing orbit plane. The nodal regression rate of the orbit line of nodes is given in ref. 6 by

$$\dot{\Omega} = \frac{-3}{2} J_2 \sqrt{\frac{GM}{a}} \left(\frac{R_e^2}{a^3}\right) \left(\frac{1}{1-e^2}\right)^2 \cos i, \tag{26}$$

where $J_2 = 1.082 \times 10^{-3}$ is the coefficient of the second harmonic term in the earth's gravitational potential. (A more exact equation for nodal

regression, also given in ref. 6, contains terms three orders of magnitude smaller than Eq. (26) and will not be required in this analysis.) The right ascension of the orbit line of nodes will now be written $\Omega = \Omega_0 + \dot{\Omega}t$, where Ω_0 is the value of Ω at the time of injection into orbit. Figure 3 shows a typical configuration for a near polar orbit right after injection. Here, δ_p is an error angle between the initial orbit line of nodes and the projection of the gyro spin axis on the earth's equatorial plane. It will be seen that the gravity gradient precession depends on this angle and on the regression rate, $\dot{\Omega}$.

From Fig. 3 it can be seen that

$$\Omega_0 - \varphi = \frac{\pi}{2} - \delta_p,$$

and, therefore,

$$\Omega - \varphi = \dot{\Omega}t + \frac{\pi}{2} - \delta_p.$$

Now,

$$\cos(\Omega-\varphi) = \sin(\delta_p - \dot{\Omega}t)$$

$$\sin(\Omega-\varphi) = \cos(\delta_p - \dot{\Omega}t).$$

Also, assuming that $i = \frac{\pi}{2} + i'$, where i' is a small error in orbital inclination, we have

$$\cos\theta = \sin\epsilon \sin(\delta_p - \dot{\Omega}t) - i' \cos\epsilon.$$

Equations (19) and (20) now become

$$\tilde{\varphi} = \Lambda\left[\cos\epsilon \sin^2(\delta_p - \dot{\Omega}t) - i' \frac{\cos 2\epsilon}{\sin\epsilon} \sin(\delta_p - \dot{\Omega}t)\right.$$
$$\left. - i'^2 \cos\epsilon\right] \tag{27}$$

$$\tilde{\epsilon} = \Lambda\left[\frac{1}{2}\sin\epsilon \sin(2\delta_p - 2\dot{\Omega}t) - i' \cos\epsilon \cos(\delta_p - \dot{\Omega}t)\right] \tag{28}$$
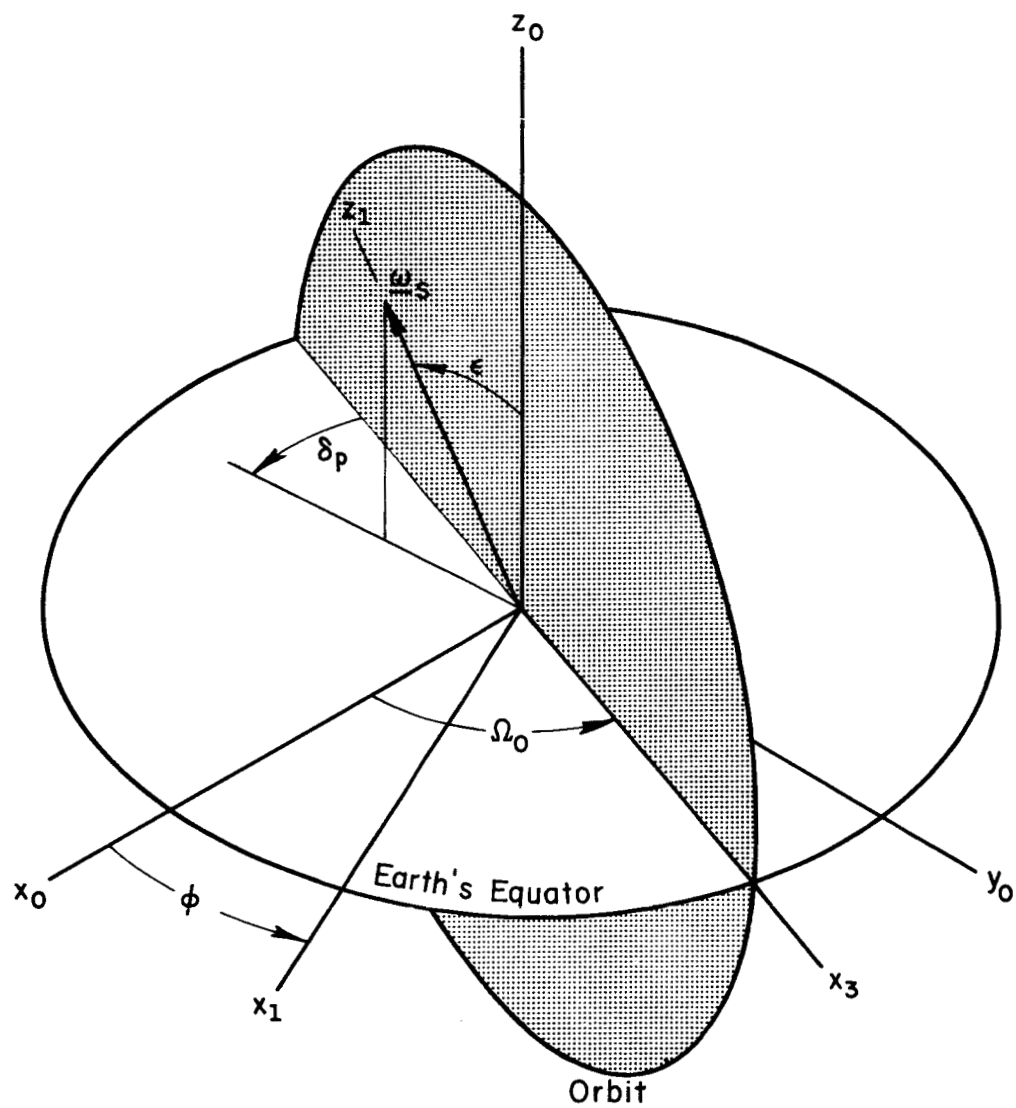
Fig. 3   Initial conditions for polar orbit.

These equations may be integrated with respect to time to give $\Delta\varphi$ and $\Delta\epsilon$ as functions of time:

$$\Delta\varphi = \frac{\Lambda}{2}\, t\, \left\{\cos\epsilon\left[1 - \sin 2\delta_p \left(\frac{1-\cos 2\dot\Omega t}{2\dot\Omega t}\right)\right.\right.$$

$$\left.\left. - \cos 2\delta_p \frac{\sin 2\dot\Omega t}{2\dot\Omega t}\right] + 2i'\,\frac{\cos 2\epsilon}{\sin\epsilon}\left[\cos\delta_p \left(\frac{1-\cos\dot\Omega t}{\dot\Omega t}\right)\right.\right.$$

$$\left.\left. - \sin\delta_p \frac{\sin\dot\Omega t}{\dot\Omega t}\right] - i'^2 \cos\epsilon\right\} \tag{29}$$

$$\Delta\epsilon = \frac{\Lambda}{2}\, t\, \left\{\sin\epsilon\left[\sin 2\delta_p \frac{\sin 2\dot\Omega t}{2\dot\Omega t}\right.\right.$$

$$\left.\left. - \cos 2\delta_p \left(\frac{1-\cos 2\dot\Omega t}{2\dot\Omega t}\right)\right]\right.$$

$$\left. - 2i'\cos\epsilon\left[\sin\delta_p \left(\frac{1-\cos\dot\Omega t}{\dot\Omega t}\right) + \cos\delta_p \frac{\sin\dot\Omega t}{\dot\Omega t}\right]\right\}. \tag{30}$$

If ϵ is allowed to vanish, these equations may give misleading results. In particular, Eq. (29) implies that $\Delta\varphi$ increases without limit as $\epsilon \to 0$. However, it must be remembered that φ and, therefore, $\Delta\varphi$, are undefined if $\epsilon = 0$ because the gyro spin axis becomes coincident with the z_o- axis, as can be seen in Fig. 3.

It will be seen later, that for practical purposes, the nodal regression rate, $\dot\Omega$, should be less than 45 degrees per year and, therefore, Eq. (26) indicates that for 400-700 mi orbits, i' must be no larger than 1° or .017 radian. Consequently, for such slow regression rates, Eqs. (29) and (30) may be simplified by dropping the terms containing i'. The simplified expressions are

$$\Delta \varphi = \frac{\Lambda}{2} \cos \in \left[1 - \sin 2\delta_p \left(\frac{1-\cos 2\dot{\Omega}t}{2\dot{\Omega}t} \right) - \cos 2\delta_p \frac{\sin 2\dot{\Omega}t}{2\dot{\Omega}t} \right] t \qquad (31)$$

$$\Delta \in = \frac{\Lambda}{2} \sin \in \left[\sin 2\delta_p \frac{\sin 2\dot{\Omega}t}{2\dot{\Omega}t} - \cos 2\delta_p \left(\frac{1-\cos 2\dot{\Omega}t}{2\dot{\Omega}t} \right) \right] t . \qquad (32)$$

Some typical curves are plotted in Figs. 4 and 5 to show the variations of $\Delta\varphi$ and $\Delta\in$ as functions of the initial misalignment angle, δ_p, and the nodal regression angle, $\dot{\Omega}t$. In these curves, the nondimensional parameters $\Delta\varphi/\Lambda t \cos\in$ and $\Delta\in/\Lambda t \sin\in$ have been plotted. These curves illustrate the need to keep the nodal regression rate and δ_p as small as possible to avoid large values of gravity gradient precession.
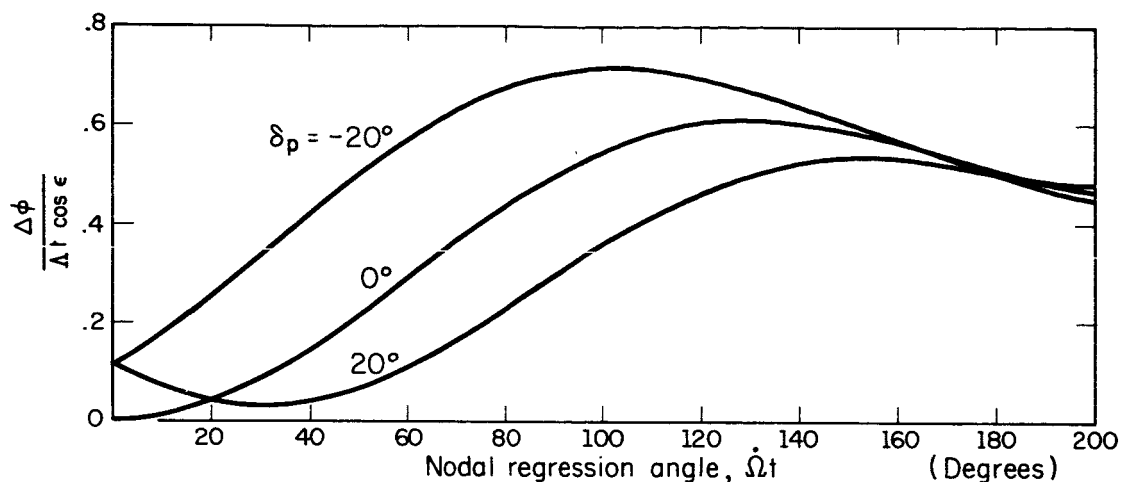
Fig. 4 Gravity gradient precession for regressing polar orbit; normalized equatorial plane component vs. regression angle.
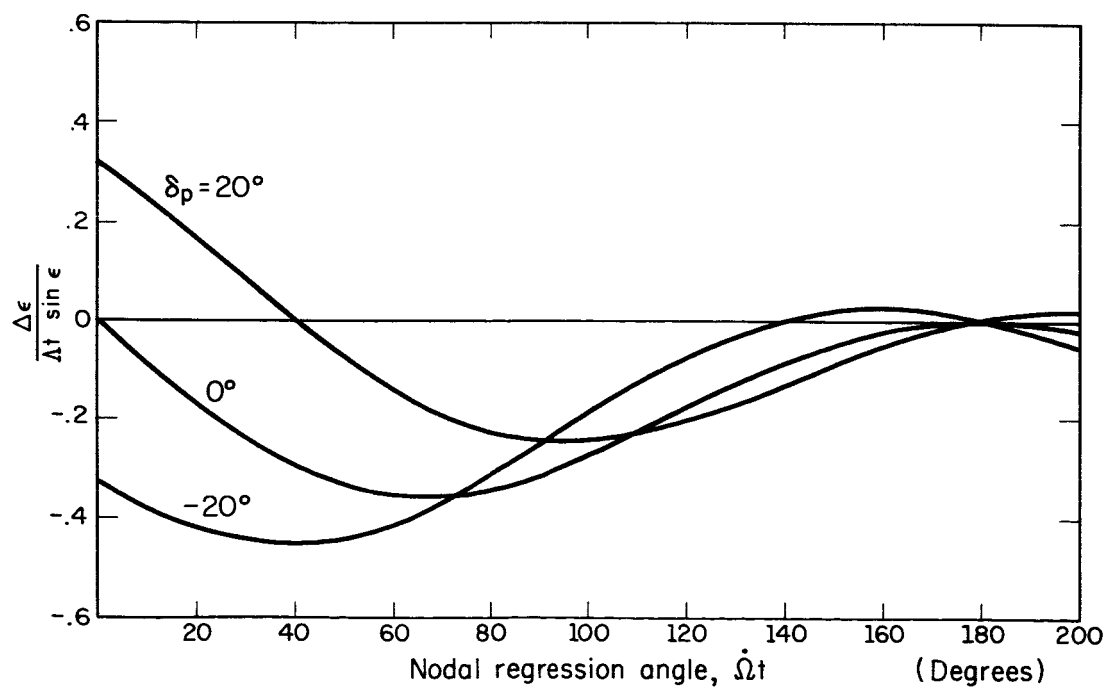
Fig. 5 Gravity gradient precession for regressing polar orbit; normalized component in plane of earth's pole and gyro spin axis vs. regression angle.

REFERENCES

1. Schiff, L. I., "Possible New Experimental Test of General Relativity Theory," Phys. Rev. Letters $\underline{4}$, 215 (March 1, 1960).

2. Schiff, L. I., "Motion of a Gyroscope According to Einstein's Theory of Gravitation," Proc. Nat. Acad. Sci., $\underline{46}$, 871 (1960).

3. Cooper, D. H., "Passive Polyhedral Gyro Satellite," Coordinated Science Laboratory Report I-128, (Feb. 16, 1965).

4. Courtney-Pratt, J. S., Hett, J. H., McLaughlin, J. W., "Optical Measurements on Telstar to Determine the Orientation of the Spin Axis and the Spin Rate," Journ SMPTE $\underline{72}$ (June, 1963).

5. Scarborough, J. B., "The Gyroscope, Theory and Applications," Interscience Publishers (1958).

6. Wolverton, R. W., (Editor), "Flight Performance Handbook for Orbital Operations," John Wiley & Sons, (1963).

7. Thomas, L. C., Cappellari, J. O. "Attitude Determination and Prediction of Spin-Stabilized Satellites," Bell System Tech. Journ. pp. 1679-80 (July, 1964).

Distribution list as of May 1, 1966

1   Dr. Edward M. Reilley
     Asst. Director (Research)
     Ofc. of Defense Res. & Engrg.
     Department of Defense
     Washington, D. C. 20301

1   Office of Deputy Director
     (Research and Information Rm 3D1037)
     Department of Defense
     The Pentagon
     Washington, D. C. 20301

1   Director
     Advanced Research Projects Agency
     Department of Defense
     Washington, D. C. 20301

1   Director for Materials Sciences
     Advanced Research Projects Agency
     Department of Defense
     Washington. D. C. 20301

1   Headquarters
     Defense Communications Agency (333)
     The Pentagon
     Washington, D. C. 20305

20 Defense Documentation Center
     Attn: TISIA
     Cameron Station, Building 5
     Alexandria, Virginia 22314

1   Director
     National Security Agency
     Attn: Librarian C-332
     Fort George G. Meade, Maryland 20755

1   Weapons Systems Evaluation Group
     Attn: Col. Finis G. Johnson
     Department of Defense
     Washington, D. C. 20305

1   National Security Agency
     Attn: R4-James Tippet
     Office of Research
     Fort George G. Meade, Maryland 20755

1   Central Intelligence Agency
     Attn: OCR/DD Publications
     Washington, D. C. 20505

1   AFRSTE
     Hqs. USAF
     Room 1D-429, The Pentagon
     Washington, D. C. 20330

1   AUL3T-9663
     Maxwell Air Force Base, Alabama 36112

1   AFFTC (FTBPP-2)
     Technical Library
     Edwards AFB, California 93523

1   Space Systems Division
     Air Force Systems Command
     Los Angeles Air Force Station
     Los Angeles, California 90045
     Attn: SSSD

1   SSD(SSTRT/Lt. Starbuck)
     AFUPO
     Los Angeles, California 90045

1   Det. #6, OAR (LOOAR)
     Air Force Unit Post Office
     Los Angeles, California 90045

1   Systems Engineering Group (RTD)
     Technical Information Reference Branch
     Attn. SEPIR
     Directorate of Engineering Standards
     & Technical Information
     Wright-Patterson AFB, Ohio 45433

1   ARL (ARIY)
     Wright-Patterson AFB, Ohio 45433

1   AFAL (AVT)
     Wright-Patterson AFB, Ohio 45433

1   AFAL (AVTE/R. D. Larson)
     Wright-Patterson AFB, Ohio 45433

1   Office of Research Analyses
     Attn: Technical Library Branch
     Holloman AFB, New Mexico 88330

2   Commanding General
     Attn: STEWS-WS-VT
     White Sands Missile Range
     New Mexico 88002

1   RADC (EMLAL-1)
     Griffiss AFB, New York 13442
     Attn: Documents Library

1   Academy Library (DFSLB)
     U. S. Air Force Academy
     Colorado 80840

1   FJSRL
     USAF Academy, Colorado 80840

---

1   APGC (PGBPS-12)
     Eglin AFB, Florida 32542

1   AFETR Technical Library
     (ETV, MU-135)
     Patrick AFB, Florida 32925

1   AFETR (ETLLG-1)
     STINFO Officer (for Library)
     Patrick AFB, Florida 32925

1   AFCRL (CRMXLR)
     AFCRL Research Library, Stop 29
     L. G. Hanscom Field
     Bedford, Massachusetts 01731

2   ESD (ESTI)
     L. G. Hanscom Field
     Bedford, Massachusetts 01731

1   AEDC (ARO, INC)
     Attn: Library/Documents
     Arnold AFS, Tennessee 37389

2   European Office of Aerospace Research
     Shell Building
     47 Rue Cantersteen
     Brussels, Belgium

5   Lt. Col. E. P. Gaines, Jr.
     Chief, Electronics Division
     Directorate of Engineering Sciences
     Air Force Office of Scientific Research
     Washington, D. C. 20333

1   U. S. Army Research Office
     Attn. Physical Sciences Division
     3045 Columbia Pike
     Arlington, Virginia 22204

1   Research Plans Office
     U. S. Army Research Office
     3045 Columbia Pike
     Arlington, Virginia 22204

1   Commanding General
     U. S. Army Materiel Command
     Attn: AMCRD-RS-PE-E
     Washington, D. C. 20315

1   Commanding General
     U. S. Army Strategic Communications Command
     Washington, D. C. 20315

1   Commanding Officer
     U. S. Army Materials Research Agency
     Watertown Arsenal
     Watertown, Massachusetts 02172

1   Commanding Officer
     U. S. Army Ballistics Research Laboratory
     Attn: V. W. Richards
     Aberdeen Proving Ground
     Aberdeen, Maryland 21005

1   Commandant
     U. S. Army Air Defense School
     Attn: Missile Sciences Division C&S Dept.
     P. O. Box 9390
     Fort Bliss, Texas 79916

1   Commanding General
     U. S. Army Missile Command
     Attn: Technical Library
     Redstone Arsenal, Alabama 35809

1   Commanding General
     Frankford Arsenal
     Attn: SMUFA-L6000 (Dr. Sidney Ross)
     Philadelphia, Pennsylvania 19137

1   U. S. Army Munitions Command
     Attn: Technical Information Branch
     Picatinney Arsenal
     Dover, New Jersey 07801

1   Commanding Officer
     Harry Diamond Laboratories
     Attn: Mr. Berthold Altman
     Connecticut Avenue & Van Ness Street N. W.
     Washington, D. C. 20438

1   Commanding Officer
     U. S. Army Security Agency
     Arlington Hall
     Arlington, Virginia 22212

1   Commanding Officer
     U. S. Army Limited War Laboratory
     Attn: Technical Director
     Aberdeen Proving Ground
     Aberdeen, Maryland 21005

1   Commanding Officer
     Human Engineering Laboratories
     Aberdeen Proving Ground, Maryland 21005

1   Director
     U. S. Army Engineer Geodesy, Intelligence
     and Mapping
     Research and Development Agency
     Fort Belvoir, Virginia 22060

---

1   Commandant
     U. S. Army Command and General Staff College
     Attn: Secretary
     Fort Leavenworth, Kansas 66270

1   Dr. H. Robl, Deputy Chief Scientist
     U. S. Army Research Office (Durham)
     Box CM, Duke Station
     Durham, North Carolina 27706

1   Commanding Officer
     U. S. Army Research Office (Durham)
     Attn: CRD-AA-IP (Richard O. Ulsh)
     Box CM, Duke Station
     Durham, North Carolina 27706

1   Superintendent
     U. S. Army Military Academy
     West Point, New York 10996

1   The Walter Reed Institute of Research
     Walter Reed Medical Center
     Washington, D. C. 20012

1   Commanding Officer
     U. S. Army Electronics R&D Activity
     Fort Huachuca, Arizona 85163

1   Commanding Officer
     U. S. Army Engineer R&D Laboratory
     Attn: STINFO Branch
     Fort Belvoir, Virginia 22060

1   Commanding Officer
     U. S. Army Electronics R&D Activity
     White Sands Missile Range, New Mexico 88002

1   Dr. S. Benedict Levin, Director
     Institute for Exploratory Research
     U. S. Army Electronics Command
     Fort Monmouth, New Jersey 07703

1   Director
     Institute for Exploratory Research
     U. S. Army Electronics Command
     Attn: Mr. Robert O. Parker, Executive
         Secretary, JSTAC (AMSEL-XL-D)
     Fort Monmouth, New Jersey 07703

1   Commanding General
     U. S. Army Electronics Command
     Fort Monmouth, New Jersey 07703

     Attn: AMSEL-SC
              RD-D
              RD-G
              RD-GF
              RD-MAF-I
              RD-MAT
              XL-D
              XL-E
              XL-C
              XL-S
              HL-D
              HL-L
              HL-J
              HL-P
              HL-O
              HL-R
              NL-D
              NL-A
              NL-P
              NL-R
              NL-S
              KL-D
              KL-E
              KL-S
              KL-T
              VL-D
              WL-D

3   Chief of Naval Research
     Department of the Navy
     Washington, D. C. 20360
     Attn: Code 427

4   Chief, Bureau of Ships
     Department of the Navy
     Washington, D. C. 20360

3   Chief, Bureau of Weapons
     Department of the Navy
     Washington, D. C. 20360

2   Commanding Officer
     Office of Naval Research Branch Office
     Box 39, Navy No. 100 F.P.O.
     New York, New York 09510

3   Commanding Officer
     Office of Naval Research Branch Office
     219 South Dearborn Street
     Chicago, Illinois 60604

1   Commanding Officer
     Office of Naval Research Branch Office
     1030 East Green Street
     Pasadena, California

1   Commanding Officer
     Office of Naval Research Branch Office
     207 West 24th Street
     New York, New York 10011

Distribution list as of May 1, 1966 (cont'd.)

1   Commanding Officer
Office of Naval Research Branch Office
495 Summer Street
Boston, Massachusetts 02210

8   Director, Naval Research Laboratory
Technical Information Officer
Washington, D. C.
Attn: Code 2000

1   Commander
Naval Air Development and Material Center
Johnsville, Pennsylvania 18974

2   Librarian
U. S. Naval Electronics Laboratory
San Diego, California 95152

1   Commanding Officer and Director
U. S. Naval Underwater Sound Laboratory
Fort Trumbull
New London, Connecticut 06840

1   Librarian
U. S. Navy Post Graduate School
Monterey, California

1   Commander
U. S. Naval Air Missile Test Center
Point Magu, California

1   Director
U. S. Naval Observatory
Washington, D. C.

2   Chief of Naval Operations
OP-07
Washington, D. C.

1   Director, U. S. Naval Security Group
Attn: G43
3801 Nebraska Avenue
Washington, D. C.

2   Commanding Officer
Naval Ordnance Laboratory
White Oak, Maryland

1   Commanding Officer
Naval Ordnance Laboratory
Corona, California

1   Commanding Officer
Naval Ordnance Test Station
China Lake, California

1   Commanding Officer
Naval Avionics Facility
Indianapolis, Indiana

1   Commanding Officer
Naval Training Device Center
Orlando, Florida

1   U. S. Naval Weapons Laboratory
Dahlgren, Virginia

1   Weapons Systems Test Division
Naval Air Test Center
Patuxtent River, Maryland
Attn: Library

1   Mr. Charles F. Yost
Special Assistant to the Director of Research
National Aeronautics and Space Administration
Washington, D. C. 20546

1   Dr. H. Harrison, Code RRE
Chief, Electrophysics Branch
National Aeronautics and Space Administration
Washington, D. C. 20546

1   Goddard Space Flight Center
National Aeronautics and Space Administration
Attn: Library, Documents Section Code 252
Greenbelt, Maryland 20771

1   NASA Lewis Research Center
Attn: Library
21000 Brookpark Road
Cleveland, Ohio 44135

1   National Science Foundation
Attn: Dr. John R. Lehmann
Division of Engineering
1800 G Street, N. W.
Washington, D. C. 20550

1   U. S. Atomic Energy Commission
Division of Technical Information Extension
P. O. Box 62
Oak Ridge, Tennessee 37831

1   Los Alamos Scientific Laboratory
Attn: Reports Library
P. O. Box 1663
Los Alamos, New Mexico 87544

2   NASA Scientific & Technical Information Facility
Attn: Acquisitions Branch (S/AK/DL)
P. O. Box 33
College Park, Maryland 20740

1   Director
Research Laboratory of Electronics
Massachusetts Institute of Technology
Cambridge, Massachusetts 02139

1   Polytechnic Institute of Brooklyn
55 Johnson Street
Brooklyn, New York 11201
Attn: Mr. Jerome Fox
Research Coordinator

1   Director
Columbia Radiation Laboratory
Columbia University
538 West 120th Street
New York, New York 10027

1   Director
Coordinated Science Laboratory
University of Illinois
Urbana, Illinois 61801

1   Director
Stanford Electronics Laboratories
Stanford University
Stanford, California

1   Director
Electronics Research Laboratory
University of California
Berkeley 4, California

1   Director
Electronic Sciences Laboratory
University of Southern California
Los Angeles, California 90007

1   Professor A. A. Dougal, Director
Laboratories for Electronics and
Related Sciences Research
University of Texas
Austin, Texas 78712

1   Division of Engineering and Applied Physics
210 Pierce Hall
Harvard University
Cambridge, Massachusetts 02138

1   Aerospace Corporation
P. O. Box 95085
Los Angeles, California 90045
Attn: Library Acquisitions Group

1   Professor Nicholas George
California Institute of Technology
Pasadena, California

1   Aeronautics Library
Graduate Aeronautical Laboratories
California Institute of Technology
1201 E. California Boulevard
Pasadena, California 91109

1   Director, USAF Project RAND
Via: Air Force Liaison Office
The RAND Corporation
1700 Main Street
Santa Monica, California 90406
Attn: Library

1   The Johns Hopkins University
Applied Physics Laboratory
8621 Georgia Avenue
Silver Spring, Maryland
Attn: Boris W. Kuvshinoff
Document Librarian

1   Hunt Library
Carnegie Institute of Technology
Schenley Park
Pittsburgh, Pennsylvania 15213

1   Dr. Leo Young
Stanford Research Institute
Menlo Park, California

1   Mr. Henry L. Bachmann
Assistant Chief Engineer
Wheeler Laboratories
122 Cuttermill Road
Great Neck, New York

1   University of Liege
Electronic Department
Mathmatics Institute
15, Avenue Des Tilleuls
Val-Benoit, Liege
Belgium

1   School of Engineering Sciences
Arizona State University
Tempe, Arizona

1   University of California at Los Angeles
Department of Engineering
Los Angeles, California

1   California Institute of Technology
Pasadena, California
Attn: Documents Library

1   University of California
Santa Barbara, California
Attn: Library

1   Carnegie Institute of Technology
Electrical Engineering Department
Pittsburgh, Pennsylvania

1   University of Michigan
Electrical Engineering Department
Ann Arbor, Michigan

1   New York University
College of Engineering
New York, New York

1   Syracuse University
Department of Electrical Engineering
Syracuse, New York

1   Yale University
Engineering Department
New Haven, Connecticut

1   Airborne Instruments Laboratory
Deerpark, New York

1   Bendix Pacific Division
11600 Sherman Way
North Hollywood, California

1   General Electric Company
Research Laboratories
Schenectady, New York

1   Lockheed Aircraft Corporation
P. O. Box 504
Sunnyvale, California

1   Raytheon Company
Bedford, Massachusetts
Attn: Librarian

DOCUMENT CONTROL DATA R&D

(Security classification of title, body of abstract and indexing annotation must be entered when the overall report is classified)

1. ORIGINATING ACTIVITY (Corporate author)	2a. REPORT SECURITY CLASSIFICATION
University of Illinois Coordinated Science Laboratory Urbana, Illinois 61801	Unclassified 2b. GROUP

3. REPORT TITLE

THE EFFECTS OF THE NODAL REGRESSION OF THE ORBIT ON THE GRAVITY GRADIENT PRECESSION OF A GYROSCOPIC SATELLITE

4. DESCRIPTIVE NOTES (Type of report and inclusive dates)

5. AUTHOR(S) (Last name, first name, initial)

Myers, James L., Jr.

6. REPORT DATE	7a. TOTAL NO. OF PAGES	7b. NO. OF REFS.
July, 1966	19	7

8a. CONTRACT OR GRANT NO.	9a. ORIGINATOR'S REPORT NUMBER(S)
b. PROJECT NO. DA 28 043 AMC 00073(E) 20014501B31F	R-309
c.	9b. OTHER REPORT NO(S) (Any other numbers that may be assigned this report)
d.	

10. AVAILABILITY/ LIMITATION NOTICES

Distribution of this report is unlimited

11. SUPPLEMENTARY NOTES	12. SPONSORING MILITARY ACTIVITY
	Joint Services Electronics Program thru U. S. Army Electronics Command Fort Monmouth, New Jersey 07703

13. ABSTRACT

A gyroscopic satellite has been proposed for a test of the general theory of relativity in which the gyro "drift" rate to be measured is less than seven seconds of arc per year. The Coordinated Science Laboratory has proposed a simple passive gyroscope which uses sunlight reflected from mirrors to provide optical data to determine the spin axis orientation. The gravity gradient torque acting on the satellite is one of several extraneous disturbances which can cause spurious precession of the gyro spin axis. In this paper, general equations for the precession of a gyro satellite in a regressing orbit are derived. These equations may be used to specify the tolerances for initial spin axis and orbit alignments which enable an accurate measurement of the relativity effect. (Author)

DD FORM 1473 1 JAN 64

KEY WORDS	LINK A		LINK B		LINK C	
	ROLE	WT	ROLE	WT	ROLE	WT
gyroscopic satellite general theory of relativity passive gyroscope gravity gradient torque precession of the gyro spin axis						

INSTRUCTIONS

1. ORIGINATING ACTIVITY: Enter the name and address of the contractor, subcontractor, grantee, Department of Defense activity or other organization (corporate author) issuing the report.

2a. REPORT SECURITY CLASSIFICATION: Enter the overall security classification of the report. Indicate whether "Restricted Data" is included. Marking is to be in accordance with appropriate security regulations.

2b. GROUP: Automatic downgrading is specified in DoD Directive 5200.10 and Armed Forces Industrial Manual. Enter the group number. Also, when applicable, show that optional markings have been used for Group 3 and Group 4 as authorized.

3. REPORT TITLE: Enter the complete report title in all capital letters. Titles in all cases should be unclassified. If a meaningful title cannot be selected without classification, show title classification in all capitals in parenthesis immediately following the title.

4. DESCRIPTIVE NOTES: If appropriate, enter the type of report, e.g., interim, progress, summary, annual, or final. Give the inclusive dates when a specific reporting period is covered.

5. AUTHOR(S): Enter the name(s) of author(s) as shown on or in the report. Enter last name, first name, middle initial. If military, show rank and branch of service. The name of the principal author is an absolute minimum requirement.

6. REPORT DATE: Enter the date of the report as day, month, year; or month, year. If more than one date appears on the report, use date of publication.

7a. TOTAL NUMBER OF PAGES: The total page count should follow normal pagination procedures, i.e., enter the number of pages containing information.

7b. NUMBER OF REFERENCES: Enter the total number of references cited in the report.

8a. CONTRACT OR GRANT NUMBER: If appropriate, enter the applicable number of the contract or grant under which the report was written.

8b, 8c, & 8d. PROJECT NUMBER: Enter the appropriate military department identification, such as project number, subproject number, system numbers, task number, etc.

9a. ORIGINATOR'S REPORT NUMBER(S): Enter the official report number by which the document will be identified and controlled by the originating activity. This number must be unique to this report.

9b. OTHER REPORT NUMBER(S): If the report has been assigned any other report numbers (either by the originator or by the sponsor), also enter this number(s).

10. AVAILABILITY/LIMITATION NOTICES: Enter any limitations on further dissemination of the report, other than those imposed by security classification, using standard statements such as:

  (1) "Qualified requesters may obtain copies of this report from DDC."

  (2) "Foreign announcement and dissemination of this report by DDC is not authorized."

  (3) "U. S. Government agencies may obtain copies of this report directly from DDC. Other qualified DDC users shall request through

                                                  ."

  (4) "U. S. military agencies may obtain copies of this report directly from DDC. Other qualified users shall request through

                                                  ."

  (5) "All distribution of this report is controlled. Qualified DDC users shall request through

                                                  ."

If the report has been furnished to the Office of Technical Services, Department of Commerce, for sale to the public, indicate this fact and enter the price, if known.

11. SUPPLEMENTARY NOTES: Use for additional explanatory notes.

12. SPONSORING MILITARY ACTIVITY: Enter the name of the departmental project office or laboratory sponsoring (paying for) the research and development. Include address.

13. ABSTRACT: Enter an abstract giving a brief and factual summary of the document indicative of the report, even though it may also appear elsewhere in the body of the technical report. If additional space is required, a continuation sheet shall be attached.

It is highly desirable that the abstract of classified reports be unclassified. Each paragraph of the abstract shall end with an indication of the military security classification of the information in the paragraph, represented as (TS), (S), (C), or (U).

There is no limitation on the length of the abstract. However, the suggested length is from 150 to 225 words.

14. KEY WORDS: Key words are technically meaningful terms or short phrases that characterize a report and may be used as index entries for cataloging the report. Key words must be selected so that no security classification is required. Identifiers, such as equipment model designation, trade name, military project code name, geographic location, may be used as key words but will be followed by an indication of technical context. The assignment of links, roles, and weights is optional.

DD FORM 1473
1 JAN 64